ISBN: 978-3-95450-216-5 doi:10.18429/JACoW-eeFACT2018-TUOAB02

LOW-EMITTANCE TUNING FOR CIRCULAR COLLIDERS

T.K. Charles*[12], S. Aumon[3], B. Holzer[1], K. Oide[14], T. Tydecks[1], F. Zimmermann[1],
[1] European Organization for Nuclear Research (CERN), Geneva, Switzerland
[2] School of Physics, University of Melbourne, 3010, Victoria, Australia
[3] ADAM SA (Applications of Detector and Accelerators to Medicine), Geneva, Switzerland
[4] KEK, Oho, Tsukuba, Ibaraki 305-0801, Japan

Abstract

The 100 km FCC-ee e+/e- circular collider requires luminosities in the order of 10^{35} cm^{-2} s^{-1} and very low emittances of 0.27 nm·rad for the horizontal plane and 1 pm·rad in the vertical. In order to reach these requirements, extreme focusing of the beam is needed in the interaction regions, leading to a vertical beta function of 0.8 mm at the IP. These challenges make the FCC-ee design particularly susceptible to misalignment and field errors. This paper describes the tolerance of the machine to magnet alignment errors and the effectiveness of optics and orbit correction methods that were implemented in order to bring the vertical dispersion to acceptable values, which in turn limits the vertical emittance. Thousands of misalignment and error seeds were introduced in MADX simulations and a comprehensive correction strategy, which includes macros based upon Dispersion Free Steering (DFS), linear coupling correction based on Resonant Driving Terms (RDTs) and response matrices, was implemented. The results are summarized in this paper.

INTRODUCTION

Electron-positron circular colliders profit from small vertical beam size due to vertical emittances close to the quantum excitation. The light source community has propelled the drive for smaller and smaller vertical emittances [1,2]. Many of the lessons learned can be applied to circular electron-positron colliders in their strive for higher luminosity.

The Future Circular Collider (FCC) will have four energies of operation ranging from the Z-pole (45.6 GeV=beam) to the $t\bar{t}$ production threshold (182.5 GeV=beam) [3]. A summary of the key parameters can be found in Table 1 and in the upcoming Conceptual Design Report (CRD).

In order to produce a high luminosity, extreme focusing is required at the interaction regions. With this comes challenging optics parameters. For the Z resonance, a vertical β^* of 0.8 mm, and a vertical emittance of 1 pm·rad is required, for a luminosity of 230×10^{34} cm^{-2}s^{-1}. Within the final focusing region, the maximum values of the beta functions $\beta_{x,\mathrm{max}} = 1587.97$ m and $\beta_{y,\mathrm{max}} = 6971.55$ m (see Fig. 1).

These large beta values, and the strong sextupoles required for chromaticity correction, make the machine extremely sensitive to magnet misalignments and field errors.

The two main sources of vertical emittance growth are coupling between the transverse planes and residual vertical dispersion. The betatron coupling poses a large threat due to the small emittance ratio (or coupling ratio) of $\epsilon_y/\epsilon_x = 0.27$ % (for the Z energy). The vertical dispersion grows the vertical emittance in accordance with the equilibrium emittance equation,

$$\epsilon_y = \left(\frac{dp}{p}\right)^2 (\gamma D_y^2 + 2\alpha D_y D_y' + \beta D_y'^2) \qquad (1)$$

where D_y is the vertical dispersion, D_y' is the derivative of the dispersion with respect to s, dp/p is the momentum spread, and γ, α and β are the usual Twiss parameters.

Generally the smaller the value of the beta function at the IP, β_y*, the larger the chromaticity, and the stronger the chromaticity correction required [4]. The sextupole magnets employed for this chromaticity correction introduce nonlinearities in the ring, which can lead to difficulties in performing the correction schemes that are outlined in the next section. This is because the correction techniques are inherently linear. If the beam is directed off-axis through the sextupole magnets, the effect to the beam seeing a skew quadrupole field, unaccounted for in the correction schemes.

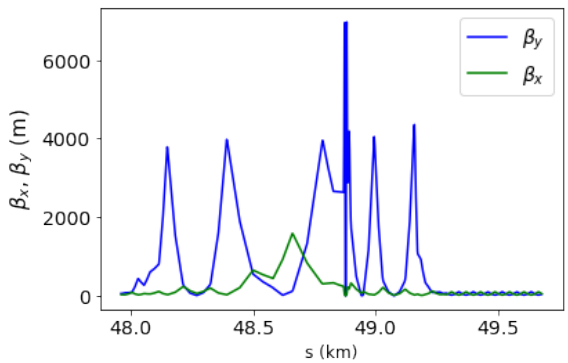

Figure 1: Beta functions near one of the IPs for the 182.5 GeV lattice. The maximum values of the beta functions $\beta_{x,\mathrm{max}} = 1587.97$ m and $\beta_{y,\mathrm{max}} = 6971.55$ m.

Table 1: Baseline beam parameters of the four operational energies for FCCee [3].

Parameters	Z	W	H	$t\bar{t}$
Beam Energy [GeV]	45.6	80	120	182.5
ϵ_x [nm·rad]	0.27	0.28	0.63	1.45
ϵ_y [pm·rad]	1	1	1.3	2.7
Beam current [mA]	1390	147	29	5.4
$\mathcal{L}$ [10^{34}cm^{-2}s^{-1}]	230	32	8	1.5

* tessa.charles@cern.ch

ISBN: 978-3-95450-216-5 doi:10.18429/JACoW-eeFACT2018-TUOAB02

Initial Assessment of Errors

Small misalignment errors were introduced and the resulting effect of vertical dispersion and the vertical orbit were measured. These results, which are summarized in Table 2, indicate that arc quadrupole vertical misalignment has the largest influence on the vertical dispersion. Introducing an error of only 2 μm randomly Gaussian distributed around the ring, will increase the maximum vertical dispersion to 326.71 mm.

Figure 2 shows the distribution of the vertical dispersions for 100 difference seeds, resulting from quadrupole vertical misalignements of 2 μm and then sextupole vertical misalignements of 10 μm.

Vertical quadrupole misalignments result in vertical closed orbit distortion which can generate vertical emittance growth from vertical dispersion, as well as vertical emittance growth from betatron coupling coming from vertical beam misalignment in the sextupoles.

Table 2: Increase (from zero) of the vertical closed orbit and vertical dispersion due to small misalignments and roll angles of individual magnetic elements, to indicate the severity of the errors introduced by various magnets.

Error type	$y_{\max}$ (mm)	$D_{y,\mathrm{rms}}$ (mm)
quad arc (Δy = 2 μm)	8.809	**326.71**
quad arc (Δx = 10 μm)	0.0	0.0
quad arc ($\Delta\phi$ = 10 μrad)	0.0	2.677
sextupoles (Δy = 10 μm)	0.0245	**57.13**
sextupoles (Δx = 10 μm)	0.0	0.0
sextupoles ($\Delta\phi$ = 10 μrad)	0.0	0.004

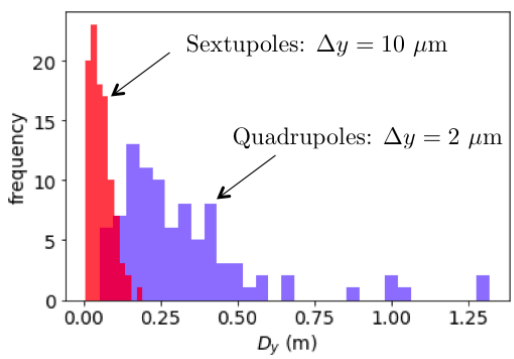

Figure 2: Distribution of vertical dispersion introduced from small sextupole and quadrupole misalignment of Δy = 2 μm for the quadrupoles and Δy = 10 μm for the sextupoles.

CORRECTION METHODS

Reducing the x-y coupling and residual vertical dispersion over the ring are key to minimizing the vertical emittance and reaching high luminosity. The correction methods implemented (in addition to orbit correction) to achieve this are Dispersion Free Steering (DFS), coupling correction and beta-beat correction.

The following subsections briefly outline the main components of the correction techniques used.

Table 3 summarizes the magnet misalignment and roll errors used in the simulations presented in the following sections. The values quoted in Table 3 are the standard derivation of the error applied through a Gaussian distribution with a random seed.

Corrector magnets and Beam Position Monitors (BPMs) are installed at every quadrupole magnet, tallying 1598 in the horizontal plane and 1596 in the vertical plane, around the 100 km ring. One skew quadrupole and one trim quadrupole are installed at every sextupole magnet for dispersion free steering and beta beat correction.

Dispersion Free Steering

DFS aims to correct the orbit and dispersion simultaneously, and in doing do effectively overcomes the sensitivity to BPM offsets. The method, which was used at LEP [5], is based upon response matrices relating the orbit, y and dispersion, D_y to the corrector kick, θ;

$$\begin{pmatrix}(1-\alpha)\vec{y}\\ \alpha\vec{D}_y\end{pmatrix} + \begin{pmatrix}(1-\alpha)\mathbf{A}\\ \alpha\mathbf{B}\end{pmatrix}\vec{\theta}$$

where $\mathbf{A}$ and $\mathbf{B}$ are the responses matrices of the orbit and the dispersion due to a corrector kick, and α is a weight factor, which can shift the emphases to or from correcting the vertical orbit or the vertical dispersion. A singular value decomposition (SVD) of the responses matrices can be written as,

$$\mathbf{A} = \mathbf{U}\mathbf{W}\mathbf{V}^{\mathrm{T}} \tag{2}$$

where the columns of $\mathbf{U}$ are the eigenvectors of $\mathbf{A}\mathbf{A}^{\mathrm{T}}$, and $\mathbf{V}$ are the eigenvectors of $\mathbf{A}^{\mathrm{T}}\mathbf{A}$ and $\mathbf{W}$ is a diagonal matrix of singular values, w_i. The tolerance or cutoff, can be applied with the SVD-method to optimize the efficiency of the calculation. More singular values moves the emphasis to more local correction but more noise, while less singular values will put the emphasis onto more global correction [6].

DFS efficiently reduces the vertical dispersion and the orbit, even in cases where the maximum weight (α = 1) is applied on the dispersion. This is convenient for machines very sensitive to BPM reading errors.

The scale of the vertical dispersion before correction is extremely large. The Root Mean Square (RMS) value before correction is 261.1 m. After applying a series of correction methods which includes orbit correction and coupling correction and DFS, the final RMS vertical dispersion at full sextupole strength, is 1.02 mm.

Coupling

Coupling introduced by sextupole misalignment and rolled quadrupoles, can be counteracted through skew quadrupoles installed at every sextupole magnet.

ISBN: 978-3-95450-216-5 doi:10.18429/JACoW-eeFACT2018-TUOAB02

Coupling between the horizontal and vertical planes need to be limited to below 0.1 %, not only in order to ensure the equilibrium vertical emittance is small, but also in order to reduced beam-beam blow up thought to be enlarged when the coupling ratio is greater than 0.1 % [7–9].

The coupling effect can be quantified through two coupling Resonant Driving Terms (RDTs) f_{1001} and f_{1010}. The analytical form of these two terms are:

$$f_{1010}^{1001} = \frac{\sum_w J_e \sqrt{\beta_x^w \beta_y^w} e^{i(\Delta\phi_{w,x} \pm \Delta_{w,y})}}{4(1 - e^{2pii(Q_u \pm Q_v)})} \quad (3)$$

where J is the vector of the skew strength, β_x^w and β_y^w are the horizontal and vertical beta functions at the location of the skew strength, and $\Delta\phi_{w,x}$ and $\Delta_{w,y}$ are the phase advances between the observation point and the skew component in the x and y plane respectively.

A response matrix, $\mathbf{M}$ of the RDTs can be written to measure the response of the RDTs to a skew quadrupole field, $\vec{\mathbf{J}}$. The system, which can be inverted via SVD, is [10]:

$$\begin{pmatrix} \vec{f_{1001}} \\ \vec{f_{1010}} \end{pmatrix}_{meas} = -\mathbf{M}\,\vec{\mathbf{J}}$$

where $\vec{f_{1001}}$ and $\vec{f_{1010}}$ are the complex coupling RDTs computed at the BPM locations.

Beta-beta Correction

Beta-beating introduced by offset sextupole magnets and quadrupole field errors, can compromise the value of β^* and reduce the achievable luminosity.

Trim quadrupole fields installed at the sextupole magnets can be used to counteract beta-beating. A response matrix method is used in two stages. Firstly, a response matrix calculated the response of the change in phase advance between the sextupoles where the trim quardupoles are installed [11]. And in a second response matrix a beta-beating response matrix is measured and the correction applied with a weighted SVD [12].

It has been previously shown [13] that correction of the phase advance is as effective as correcting the actual beta function, and therefore the phase-beating between consecutive BPMs can be used.

For n trim quadrupoles which can exercise a small field strength k_1, the weighted SVD can be applied through adding weighting factors f to each measurement of the beta-beat.

$$\begin{pmatrix} f_1\left(\frac{\beta_1-\beta_{y0}}{\beta_{y0}}\right) \\ f_2\left(\frac{\beta_2-\beta_{y0}}{\beta_{y0}}\right) \\ \dots \\ f_m\left(\frac{\beta_m-\beta_{y0}}{\beta_{y0}}\right) \end{pmatrix}_{meas} = \begin{pmatrix} f_1\,(R_{11}, R_{12}, R_{13}, \dots, R_{1n}) \\ f_2\,(R_{21}, R_{22}, R_{23}, \dots, R_{1n}) \\ \dots \\ f_m\,(R_{m1}, R_{m2}, R_{m3}, \dots, R_{mn}) \end{pmatrix} * \begin{pmatrix} k_1 \\ k_2 \\ \dots \\ k_n \end{pmatrix}$$

where β_{y0} is the ideal beta function at the given BPM, $R_{i,j}$ are elements in the response matrix.

The weighted SVD can provide additional emphasis on the quadrupoles where large values of the beta function are expected. In our case, a weighting factor of 10 was applied to the quadrupoles where the design value of the β_y was above 3000 m, and for every other quadrupole, the weight factor was unity. By doing this, we can ensure more accurate beta-beat correction at the location of the IP.

Figure 3 shows the iterative application of the weighted SVD approach showing a gradual reduction in the β-beat at the IPs.

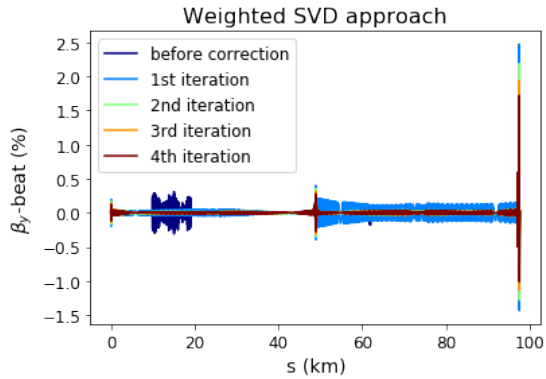

Figure 3: Weighted SVD approach, using a beta-beat response matrix and a weighted of 10 applied to the IP quadrupoles. Note s= 49 km and s= 100 km correspond to the two IPs.

CORRECTION STRATEGY

In order to minimize the equilibrium vertical emittance, a correction strategy was implemented that utilizes a number of correction schemes. Importantly the sextupole strengths are initial set to zero. This is because the initial magnet misalignment, tilts and field errors are likely to direct the beam off centre through the sextupole magnets, which has the same effect as a skew quadrupole would in its place. This results in a vertical displacement of the closed orbit with respect to the sextupole's magnetic center, and can generate vertical emittance growth through the introduction of vertical dispersion. Therefore the correction strategy begins with turning the sextupoles off. After an initial closed orbit correction, coupling correction, and beta-beat correction, the sextupole strengths are changed to 10 % of the design strength, and further orbit and optics corrections are applied and rematching of the tune. Looping through the correction strategy, increasing the sextupole strength 10 % each time, reduces the likelihood of not being able to find the closed orbit, or the risk of running into the integer or half-integer resonance. The final stage of the correction scheme includes further coupling correction to lower the vertical emittance.

All of the corrections methods were applied without RF activated and energy loss from synchrotron radiation not included. This approach allows for faster computation time and is considered valid for a fully tapered machine [14]. In the final stage of the simulations, synchrotron radiation

ISBN: 978-3-95450-216-5 doi:10.18429/JACoW-eeFACT2018-TUOAB02

Table 3: Misalignment errors introduced into the lattice before correction applied.

	σ_x (μm)	σ_y (μm)	σ_θ (μrad)
arc quadrupoles	100	100	100
IP quadrupoles	0	0	0
sextupoles	100	100	0

is turned on to compute the emittance. The emittance is calculated using the EMIT command in MADX, which is based upon the Chao formalism for equilibrium emittance calculation [15].

The following correction strategy was implemented:

1. Introduce BPMs and corrector magnets at every quadrupole, and introduce skew and trim quadrupoles at every sextupole. Misalignment and roll errors are then applied to magnets around the ring, distributed via a Gaussian distribution truncated at 2.5 sigma. Several simulations with different random seeds were used.
2. Sextupoles were turned off, and an orbit correction performed with MICADO in MADX [16].
3. Coupling correction is performed, followed by rematching of the tune, followed by beat-beat correction.
4. DFS (D_y correction) is performed followed by coupling correction (which is needed due to the change in the corrector strengths brought about by DFS). These two correction techniques are one after another.
5. Sextupoles are then set to 10% of their design strength.
   (a) orbit corrections
   (b) coupling correction
   (c) tune matching
   (d) beta beat correction
   (e) coupling + dispersion correction
   (f) increase sextupole strengths by 10% , and repeat Step 5 until 100% of design sextupole strength is reached.
6. Final correction of coupling and beat-beat correction can be applied in the final step.

CORRECTED LATTICE

After applying the correction scheme outlined in the previous section, the final emittances can be reduced to an acceptable level. Figure 4 shows the vertical dispersion before and after the correction strategy has been applied. Figure 5 shows the distribution of horizontal and vertical emittances for 500 random seeds. The mean vertical of the emittance is 0.093 pm·rad, and the horizontal emittance is 1.520 nm·rad. The ratio of the emittance (or the coupling ratio), ϵ_y/ϵ_x= 0.006 %.

Including the IP quadrupoles increase the level of difficulty in performing the correction. However a large number of seeds still converge - 700 out of 1000 seeds. For the errors

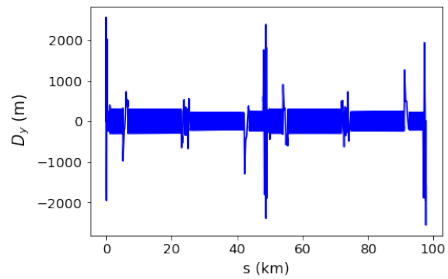

(a)

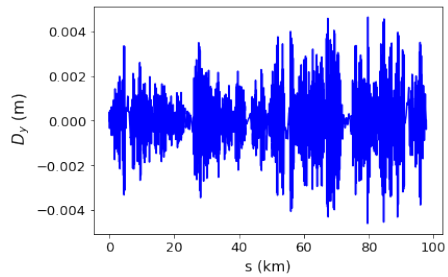

(b)

Figure 4: (a) Vertical dispersion after errors (Table 3) are introduced. Before correction the RMS vertical dispersion is 261.1 m. (b) After all correction methods applied, including DFS. The final RMS vertical dispersion is 1.02 mm.

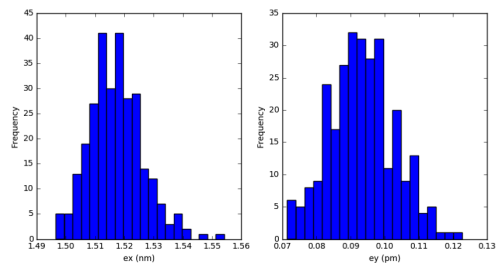

Figure 5: Distribution of vertical and horizontal emittances for the corrected lattices from many random seeds. The errors that were introduced are summarised in Table 3.

summarised in Table 4, the distribution of horizontal and vertical emittances are shown in Fig. 6.

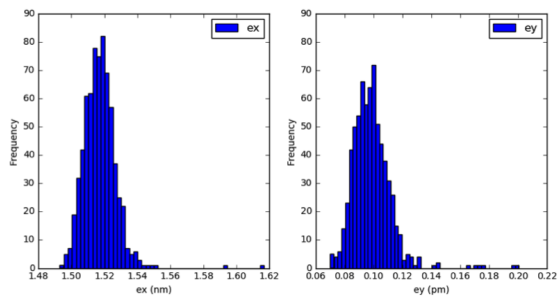

Figure 6: Distribution of vertical and horizontal emittances for the corrected lattices from many random seeds. The errors that were introduced are summarised in Table 4.

ISBN: 978-3-95450-216-5 doi:10.18429/JACoW-eeFACT2018-TUOAB02

Table 4: Misalignment errors introduced into the lattice before correction applied.

	σ_x (μm)	σ_y (μm)	σ_θ (μrad)
arc quadrupoles	100	100	100
IP quadrupoles	50	50	50
sextupoles	100	100	100

Table 5: Misalignment errors introduced into the lattice before correction applied.

	σ_x (μm)	σ_y (μm)	σ_θ (μrad)
arc quadrupoles	100	100	100
IP quadrupoles	100	100	100
sextupoles	100	100	

Finally, Fig 7 shows the resulting emittances when the tolerance of the misalignment of the IP quadrupoles is extended out to 100 μm. For this scenario 369 out of 1000 seeds converged, however the seeds that did successfully converge reached similar emittance values as to those shown in Fig. 5 and Fig. 6. Further study is underway to improve the correction strategy to increase the number of successful seeds. The mean vertical emittance in Fig. 7 is 0.11 pm·rad, and the horizontal emittance is 1.52 nm·rad. The ratio of the emittance (or the coupling ratio), ϵ_y/ϵ_x= 0.007 %.

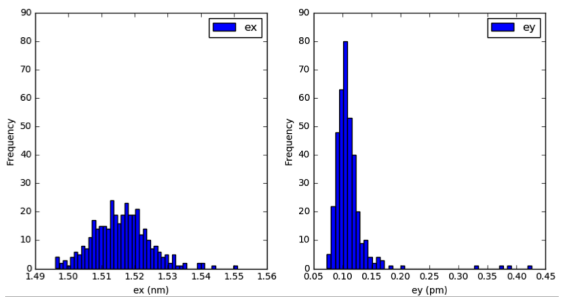

Figure 7: Distribution of vertical and horizontal emittances for the corrected lattices from many random seeds. The errors that were introduced are summarised in Table 5.

DYNAMIC APERTURE

Continuous top-up injection is mandatory for FCC-ee in order to guarantee high luminosity. Injection into a fully squeezed machine optics is therefore required. The effects of magnet misalignments on dynamic and momentum aperture were tested by means of particle tracking in MAD-X-PTC. The misalignments used in this scenario are listed in Tab. 6.

Out of 1000 seeds started for correction, 700 converged and returned with corrected optics which were then used to study the resulting apertures. In Fig. 8, the resulting dynamic and momentum apertures for the corrected machines are presented taking only radiation damping into account, whereas Fig. 9 shows the case including radiation damping and quantum excitation.

Table 6: Misalignment errors used for studying dynamic and momentum aperture.

	σ_x (μm)	σ_y (μm)	σ_θ (μrad)
arc quadrupoles	100	100	100
IP quadrupoles	50	50	50
sextupoles	100	100	

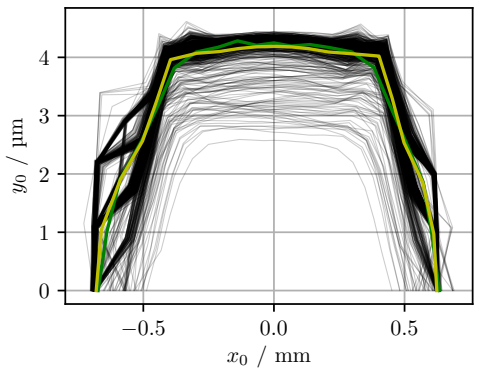

(a) Dynamic aperture

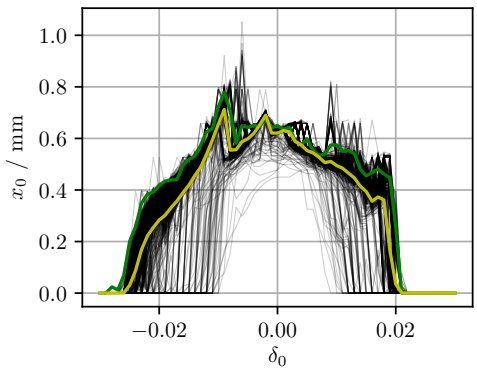

(b) Momentum aperture

Figure 8: Dynamic and momentum aperture for misaligned machine (grey), average of misaligned machines (yellow), and reference without errors (green). Simulation including radiation damping only.

Using the mean horizontal emittance of 1.52 nm rad for all seeds, and the value of horizontal aperture in Fig. 8a, the resulting aperture in multiples of horizontal beam size is approximately 16 σ_x, sufficient for injection and beam storage.

The resulting apertures show that with the set up automated correction scheme, it is possible to achieve sufficient dynamic and momentum aperture to accommodate injection and to stably store beam for most seeds.

CONCLUSION

FCC-ee present unique challenges when it comes to emittance tuning. The small values of the vertical emittance (1

ISBN: 978-3-95450-216-5 doi:10.18429/JACoW-eeFACT2018-TUOAB02

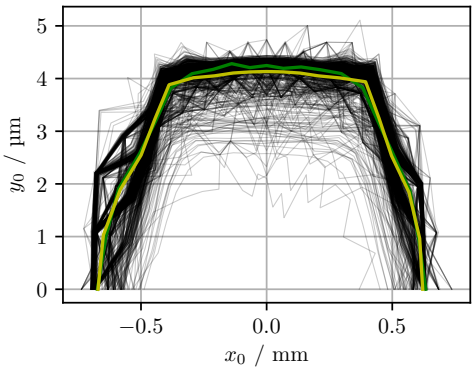

(a) Dynamic aperture

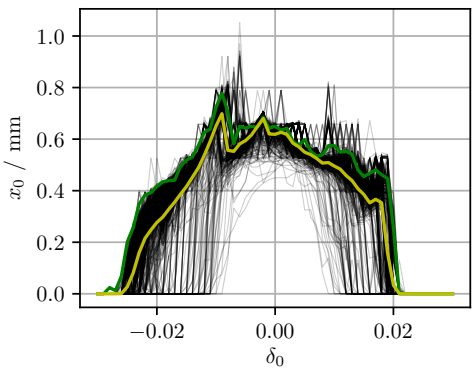

(b) Momentum aperture

Figure 9: Dynamic and momentum aperture for misaligned machine (grey), average of misaligned machines (yellow), and reference without errors (green). Simulation including radiation damping and quantum excitation.

pm·rad) and the low coupling ratio (>0.1 %) makes the FCC-ee design particularly susceptible to misalignment and field errors. This paper outlines the correction strategy approach, which includes orbit corrections, Dispersion Free Steering, linear coupling correction based on Resonant Driving Terms and beta-beat correction using response matrices. For misalignments of 100μm in x and y and a roll angle error of 100μrad, the final vertical emittance achieved is 0.11 pm·rad, and a coupling ratio of ϵ_y/ϵ_x= 0.007 %.

REFERENCES

[1] M. Aiba, M. Böge, N. Milas, and A. Streun, "Ultra low vertical emittance at SLS through systematic and random optimization," *Nucl. Instruments Methods Phys. Res. Sect. A Accel. Spectrometers, Detect. Assoc. Equip.*, **694**, pp. 133–139, 2012.

[2] R. Dowd, M. Boland, G. Leblanc, and Y. R. E. Tan, "Achievement of ultralow emittance coupling in the Australian Synchrotron storage ring," *Phys. Rev. ST AB*, **14**, 012804, 2011.

[3] K. Oide, et al, "Design of beam optics for the future circular collider e+e- collider rings," *Phys. Rev. AB*, **19**, 111005, 2016.

[4] K. Oide "Electron–Positron Circular Colliders," *Reviews of Accelerator Science and Technology Volume 7: Colliders*, World Scientific, ISBN: 978-981-4651-48-6 2015.

[5] R. W. Assmann, P. Raimondi, G. Roy, and J. Wenninger, "Emittance optimization with dispersion free steering at LEP," *Phys. Rev. ST AB*, **3**, 121001, 2000.

[6] S. Aumon, B. Holzer, K. Katsunobu A. Doblhammer, B. Haerer, "Tolerance Studies and Dispersion Free Steering for Extreme Low Emittance in the FCC-ee Project," *Proc. of IPAC2016, Busan, Korea*, **3**, THPOR001, 2016.

[7] K. Oide, D. Shatilov, S. Aumon, T. Charles, D. El Khechen, and T. Tydecks, "Several topics on Beam Dynamics in FCCee," *eeFACT 2018, Hong Kong*, These Proc., 2018.

[8] K. Oide "Optics Choices for High Luminosity IR Including Crab Waist Scheme," *eeFACT 2018, Hong Kong*, These Proc., 2018.

[9] D. El Khechen, K. Oide, F. Zimmerman "Beam Losses Due to Beam-beam and Beamstrahlung under Lattice Nonlinearity", *eeFACT 2018, Hong Kong*, These Proc., 2018. These Proc., 2018.

[10] A. Franchi, L. Farvacque, J. Chavanne, F. Ewald, B. Nash, K. Scheidt, and R. Tomás, "Vertical emittance reduction and preservation in electron storage rings via resonance driving terms correction," *Phys. Rev. ST AB*, **14**, no. 3, pp. 1–19, 2011.

[11] S. Aumon, B. Holzer, and K. Oide, "Vertical Dispersion And Betatron Coupling Correction For FCC-ee ," *Proc. of IPAC2017, Copenhagen, Denmark*, MOPIK097, 2017.

[12] C. Liu, R. Hulsart, A. Marusic, R. Michnoff, M. Minty, V. Ptitsyn, and N. York, "Weighted SVD algorithm for Closed-Orbit Correction and 10 Hz Feedback in RHIC," *Proc. IPAC2012, New Orleans, Louisiana, USA*, WEPPP084, pp. 2906–2908, 2012.

[13] R. Tomás, O. Brüning, R. Calaga, S. Fartoukh, A. Franchi, M. Giovannozzi, Y. Papaphilippou, S. Peggs, and F. Zimmermann, "Procedures and Accuracy Estimates for Beta-Beat Correction in the LHC," *Proc. EPAC06*, pp. 2023–2025, 2006.

[14] S. Aumon, B. Holzer, K. Oide, A. D. Technische, U. Wien, B. H. Kit, and B. Haerer, "Coupling and Dispersion correction for the Tolerance Study in FCC-ee," *Proc. eeFACT2016, Daresbury, UK*, pp. 151–156, 2016.

[15] A. Chao, "Evaluation of Beam Distribution Parameters in an Electron Storage Ring," *J.Appl.Phys.*, **50**, 595, pp. SLAC–PUB–2143, 1979.

[16] "Methodical Accelerator Design Manual," *http://madx.web.cern.ch*.